Paleobiology, 12(2), 1986, pp. 143–160

A biomechanical model for the morphogenesis of regular echinoid tests

Jacob Dafni

Abstract.—Experiments were conducted to test the hypothesis that biomechanical constraints determine the morphology of regular echinoids. Hard-bottom-dwelling *Tripneustes gratilla elatensis* were transferred to an artifical sandy habitat to evaluate whether the change in substrate affects their height to diameter ratio (H/D). Within 1–2 months their H/D ratio increased significantly. This change was shown to be reversible to some extent. Surgical damage to the ambulacral system of one ray caused inactivation of tubefeet and atrophy of injured ambulacra. Test shape was also affected: the damaged ray was lower, and the nondamaged ambulacra deflected toward the treated one, producing bilateral symmetry as in recorded cases of teratology. Study of *T. g. elatensis* tetramers showed that while "perfect" tetramery was apparently associated with genetic aberration, "imperfect" tetramery results from mechanical injury at an early ontogenetic stage. Micromorphological study shows that in the longitudinal sutures, normally under tension, long and slender trabeculae develop, associated with long and well-aligned collagenous sutural fibers, while the latitudinal trabeculae and fibers are short and less organized. A mechanical effect is suggested by the oval cross-section of the fiber-anchoring trabeculae. Further, echinoid plates interact like soap bubbles, whereas the entire test behaves like a balloon, fastened to the substrate by the ambulacral tubefeet. All these observations support earlier hypotheses on the biomechanical control of echinoid test growth. A model is proposed in which the expansion of the inner mass, counteracted by the mechanical activity of the ambulacral tubefeet, mesenterial threads, and lantern muscles, affects sutural growth, thus controlling echinoid morphogenesis.

A morphometric survey among regular echinoids reveals an inverse relationship between ambulacral width and relative ambital height. Although both increase of ambulacral width and lowering of ambitus-line are evolutionary trends, it is suggested that they are a response to a mechanical effect. H/D ratio was not related to ambulacral width on the phylogenetic level. It is therefore suggested that the latter correlation is ontogenetically controlled. Aspects of irregular echonoid evolution, such as bilateral symmetry, flattening, and formation of the ambulacral petaloid, also are explained by this model.

Jacob Dafni. Interuniversity Institute of Eilat, H. Steinitz Marine Biology Laboratory, P.O. Box 469, Eilat, 88103 Israel

Accepted: February 26, 1986

Introduction

Observers frequently are interested in the similarities between the morphology of living forms and inanimate mechanical structures (Thompson 1917, 1942; Raup 1968; Benson 1975; Seilacher 1979). It is generally argued that natural selection favors stable and economically efficient structures (Gutmann 1977), obtainable by following mechanical principles of design (Wainwright et al. 1976). The question whether such structures evolve phylogenetically, selected from genetically based variability, or develop phenotypically, through the daily interaction with the physico-mechanical environment, often is evaded by students of functional morphology. A probable reason is that the evidence for biomechanical influences on body shape during ontogeny is usually not sufficient to undermine the orthodox belief that morphology, like the anatomy and physiology of an organism, is inherited. Bonner (1961), attempting to link the opposing views, raised the possibility that "responsiveness to the [physical] environment is adaptively advantageous and is therefore maintained by selection."

It would seem that regular echinoids are especially susceptible to physico-mechanical constraints during morphogenesis because of their larger size and thin, relatively feeble supporting structures. Yet they exhibit high morphological stability and resistance against mechanical impact that results from a combination of tightly fitting calcareous plates and flexible sutural collagen fibers (Moss and Meehan 1967, 1968; Strathmann 1981; Telford 1985). The last author analyzed the echinoid test's mechanical de-

0094-8373/86/1202-0002/$1.00

sign and found it to be well adapted to resist external forces and load. Thompson (1917), on the other hand, emphasized the influence of internal forces on its skeletal morphology. He pointed out the resemblance between a regular echinoid's shape, calcified externally and fluid-filled internally, and that of a drop of liquid, balanced between gravitational pull of the liquid content and the outer surface tension. Suggesting that the entire test is plastic to some extent, he hypothesized that adherence of the ambulacral podia (tubefeet) to a solid substrate affects the profile of the test, causing it to become flatter. This hypothesis has been subsequently supported by field observations: individual urchins, living on soft-bottom substrates, or among seaweed, where less adhesion is afforded, tend to be taller than their hard-bottom conspecifics (Moore 1935; McPherson 1965).

A similar approach was adopted by more recent investigators. Moss and Meehan (1968) maintained that echinoid growth is induced by "expansive forces," that is, volumetric growth of the enclosed body tissues and cativies that serve as "functional organic matrix" for secondary skeletal growth. According to these authors, tensional stresses produced at the plate sutures facilitate peripheral growth of the plates. Raup (1968), on the other hand, interpreted "close-packing patterns" at the plate edge as evidence for sutural compression, that limits their growth and consequently determines the plate's shape. Further supporting this approach, Dafni and Erez (1982) showed a general correspondence between the spatial distribution of tethering contractile and elastic tissue elements and the differential calcification pattern of regular echinoid plates. Furthermore, Dafni (1980, 1983b) suggested that recently recorded skeletal deformities result from incomplete calcification that leads to perturbations in the mechanical stability of the test during growth.

More support comes from the morphology of the skeletal plates. Thompson (1917) and Raup (1968) noticed that echinoid plate-edges curve in a similar way to soap bubbles, indicating elastic behavior, but did not provide any explanation for this analogy. Relevant for test design and stability are also the mechanical properties of its microstructural components—mineral stereom and sutural collagen fibers. The various echinoid stereom types, recently reviewed by Smith (1980), differ in thickness, degree of organization of the calcareous trabeculae, and amount of fenestration, as well as in their mechanical strength (Wainwright et al. 1976; Emlet 1982). Sutural fibers also differ in density and alignment (Moss and Meehan 1967; Kobayashi and Taki 1969), in correlation with the stereom mesh organization (Smith 1980).

This paper presents evidence, obtained through experiments and observation, concerning the possible effect of mechanical forces on normal and abnormal skeletogenesis in the post larval stages of the common Red Sea echinoid *Tripneustes gratilla elatensis* Dafni (1983a). This evidence supports Thompson's hypothesis that echinoid skeletal morphology is regulated biomechanically. Experiments included transfer of living urchins to a soft-bottom artificial habitat, so disrupting the normal mechanical activity of tubefeet. Another experiment involved inflicting surgical damage on normal urchins, and observing their subsequent regneration patterns. Naturally occurring abnormal nonpentamerous individuals were also studied. The micromorphology of the test plates, cross-section of skeletal trabeculae, and length and abundance of associated collagenous fibers were quantitatively studied, and correlated with the prevalent mechanical forces.

A model is proposed to describe echinoid test growth and morphogenesis in terms of biomechanical regulation by contractile and elastic tissue elements. The generality of the model is tested in a morphometrical survey of living and extinct regular echinoid species, and by observations on the test morphology of irregular echinoids.

Material and Methods

1. Effect of tubefeet activity on test morphology

(a) To test Thompson's (1917) hypothesis that adherence of tubefeet causes urchin tests to become flatter, groups of hard-bottom-dwelling *T. g. elatensis* were maintained for extended periods on a soft substrate, at different seasons. The urchins, 10–35 mm in diameter, were collected in the subtidal zone of a wave-exposed rocky shore at Eilat (Gulf of Aqaba, Red Sea) and

placed in a shallow aquarium (1.5 m × 2 m, and 20 cm deep), layered with fine sand, gradually sloping to the rim. Seawater circulation was at ambient temperatures (23°–25°C). The urchins were fed with the alga *Ulva lactuca* (L.). Five caliper measurements were taken initially for each individual, of test horizontal diameter (D) and height (H), to the nearest 0.1 mm. The urchins were also measured at the end of the experiment, and the change in average diameter and height versus diameter (H/D) ratio was recorded. Control groups were kept in glass-bottom aquaria, under otherwise identical conditions. One experimental group was transferred back to the sea after the "sand treatment" and housed for 30 days in a rigid PVC cage, filled with algae-covered stones.

(b) The role of tubefeet activity in determining the test shape was tested also by immobilizing one of the ambulacral (amb) radii of living *T. g. elatensis*. This was performed by inserting a surgical blade through the peristome membrane, damaging the lantern retractor muscle, radial water canal, and the adjacent nerve cord. The operation was repeated 1–3 times within one month. The damaged amb was always no. V (the amb opposite to the madreporite, according to Loven's plan [Hyman 1955]). After in vivo observations, the animals were killed and their histology examined.

(c) Nonpentamerous abnormal *T. g. elatensis*, collected at various localities in the northern Gulf, were examined with a low magnification dissecting microscope, alive or after cleaning with 5% sodium hypochlorite (NaOCl) solution.

2. Plate shape, suture morphology, and microstructural observations

(a) The morphology of plate edges in *T. g. elatensis* was examined by study of plates, amb, and interambulacral (interamb), of different sizes, and by observing growth-line patterns which show clearly after cleaning with sodium hypochlorite and charring at 300°C in a muffle furnace (Pearse and Pearse 1975).

(b) Cleaned, air-dried, and gold-coated skeletal pieces were examined with a scanning electron microscope (SEM)-JEOL-JSM 35.

(c) Skeletal pieces from the aboral half of a recently killed 10-mm *T. g. elatensis* were fixed and decalcified with Zenker's fluid (Culling 1974) and embedded in paraffin. Transverse and tangential sections of amb and interamb plates were stained with Heidenhain's Azan and MSB stains (Culling 1974), so that density and abundance of the fibers at the various sutures could be studied and measured directly, using a micrometric ocular. The sutural "trabecular ghosts"—nonstained areas surrounded by the stained fibers—were also measured.

3. Morphometric evidence

A morphometric survey was conducted to test the hypothesis that a relatively wider ambulacral system, implying stronger adherence to the substrate, affects the echinoid test configuration in living and fossil regular echinoids. One hundred and fifty species, of the orders Cidaroida, Aulodonta (Diadematacea), Stirodonta, and Camarodonta, illustrated in great detail by Mortensen (1928–1943) and Moore (1966), were measured (from the illustrations) to obtain the following indices: (a) Test height/test diameter ratio; (b) Ambital position (Ambitus height/test height); and (c) relative width of the ambulacral plates at ambitus level. For several living species actual test measurements were found to be within 5% of those obtained by measuring the illustrations. Other morphological features of fossil and contemporary species were observed and correlated with information on their life habits.

Results

1. Effects of ambulacral activity

(a) Transfer to soft-bottom artificial habitat.—The urchins which were transferred to the experimental vessel showed limited mobility on the loose sand. They tended to cling to firm objects—small pebbles and algal thalli—and clustered in dense aggregations. This behavior prevailed until the sand was covered by an algal film. In the control groups aggregation occurred only during feeding.

A significant increase in the test height versus diameter (H/D) ratio was shown in all three experimental groups (Table 1A). In group III it showed in only 17 days, during which the diameter (D) had barely changed. Transfer of group III back to the original subtidal habitat, protected by a hard PVC cage, resulted with a barely significant decrease in H/D ratio within

TABLE 1. Change in test diameter, D (in mm) and height vs. diameter ratio (H/D) (means ± SD) in three experimental groups of *T. g. elatensis*, removed from their natural hard-bottom habitat into a sand-bottom aquarium (I–III). One such group (III) was transferred back to the original habitat and restricted there in a hard PVC cage. Parentheses indicate no. of survivors at the experiment's end. Three control groups (IV–VI) were maintained in hard-bottom aquaria. Means of diameter and H/D values were differentiated with a two-tailed *t*-test: *, $P < 0.1$; **, $P < 0.05$; ***, $P < 0.01$; (—), non-significant. Season: S, summer; A, autumn; W, winter.

Group	n	Initial measurements (D)	Initial measurements (H/D)	Days, season	Final measurements (D)	Final measurements (H/D)	Significance In D	Significance In H/D
Experiment A. Transfer to sand								
I	10	28.71 ± 3.14	0.529 ± 0.028	W38	30.27 ± 3.52	0.559 ± 0.034	(—)	**
II	18	10.59 ± 1.88	0.539 ± 0.034	S42	26.44 ± 3.83	0.572 ± 0.026	***	***
III	21 (19)	36.35 ± 4.10	0.537 ± 0.032	A17	36.81 ± 3.99	0.557 ± 0.031	(—)	**
Experiment B. Transfer back to the sea								
III	19 (16)	36.81 ± 3.99	0.557 ± 0.031	W30	37.75 ± 3.40	0.541 ± 0.028	(—)	*
Control groups								
IV	11	21.05 ± 4.42	0.542 ± 0.023	A70	26.36 ± 3.93	0.539 ± 0.020	***	(—)
V	15	34.93 ± 13.7	0.531 ± 0.040	W60	49.82 ± 8.17	0.528 ± 0.027	***	(—)
VI	9 (7)	36.67 ± 6.30	0.532 ± 0.012	S60	47.25 ± 3.65	0.541 ± 0.032	***	(—)

30 days (Table 1B). Although growing intensely, H/D ratio of the control groups did not change significantly.

Qualitative observations on group I urchins, held for a subsequent month in a glass aquarium, showed that they tended to decrease their high H/D ratio. Most group II urchins were killed and preserved, while several individuals, subjected to a ^{45}Ca incorporation assay, exhibited abnormal calcification patterns (Dafni and Erez, in prep.).

(b) Effect of damaging the ambulacral system.—Response to surgical injury of the ambulacral system, and observations of accidental damage, are summarized in Table 2. Of the eight treated individuals, two showed complete regeneration of the amb system, three did not survive the operation, and three showed the following changes:

One urchin (no. 1) showed reduced activity of the treated amb 2 wk after the first incision, and its tubefeet became reduced in size and relatively inactive. The activity of the other four ambs was not impaired. Post-mortem examination, 3 months after the treatment when the diameter had reached 46 mm, showed that the retractor muscles of the treated amb (V) had atrophied and its auricle pair, to which these muscles normally attach, had totally disappeared. The protractor muscles, attached to the interamb bases at both sides of the treated amb, appeared to be intact. The skeletal configuration of this urchin changed considerably (Fig. 1A): The affected column of amb plates became shorter aborally, and the uppermost plates, apparently added subsequent to the operation, were narrow latitudinally and most of them showed no tubefeet pores. This individual's apical plate system was elongated (5.8 × 3.2 mm) in the V-2 axis, that became ultimately the axis of an apparent bilateral symmetry for the entire test. Most remarkable was the deflection of the untreated ambs, I and IV, toward amb V (Fig. 1A, B). Amb V was 3 mm lower than the rest, and the entire test became skewed along the V-2 axis (Fig. 1B). Urchins 2 and 3 showed temporary loss of tactile activity in amb V, though it had been regained by no. 3 within 1 month. Post-mortem examination showed that in both individuals the retractor muscle and auricles had disappeared from the treated amb, and the test became slightly skewed along the same axis (Table 2).

Individual 4 was not treated surgically, but had had a dermal disease in the superambital region of amb I, resulting in a malfunctioning ambulacral system. Later observations, conducted for 2 months in captivity, showed that this amb's podia remained almost inactive and their suction discs were smaller than those of other ambs. In a post-mortem examination all muscles and auricles of this urchin were found to be intact. Its skeletal morphology was almost identical to that of no. 1, that is, in the affected ambulacrum the plates were small and poreless aborally, the apical disc was elongate, and the

TABLE 2. Summary of experiments and observations concerning *T. g. elatensis* tubefeet inactivation.

No.	Cat. no.	Size & H/D	Treatment or anomaly type	Consequent morphological characteristics	
				Shared features	Unique phenomena
1	468	38–46 mm	Surgical damage of amb V tubefeet system (lantern muscles, radial water canal and nerve cord).	Reduced activity of treated amb. Partial or complete atrophy of amb V retractor muscle and auricle.	Apparent bilateral symmetry: deflection of nearest ambs. Elongation of apex and skewness in V-2 axis.
2	628	23–27 mm			Slight skewness in V-2 axis
3	515	?–46 mm			Amb V tubefeet activity restored. Slight skewness in V-2 axis.
4	513	37 mm	Aboral half of amb 1 shows dermal infection and discoloration.	Amb I activity reduced. Small tubefeet discs. No auricle atrophy.	Bilateral symmetry in I-3 axis. Apex elongated in the same axis. Amb I depressed and skewed.
5	271	43 mm (0.65)	"Perfect" tetramery	Tetramerous symmetry: 4 ambs, 4-jaw lantern, 4 auricles. Apex tetramerous.	
6	302	56 mm (0.64)			
7	318	31 mm (0.60)			
8	630	29 mm (0.60)	"Imperfect" tetramery	Aborally "perfect" tetramerous. Adorally irregular: 5-jaws, 4 or 5 auricles.	One interamb ×1.3 than the rest. Small amb plate rudiments adorally.
9	629	44 mm (0.60)			Amb rudiment 4–5 plates high, retaining retractors and auricle. Highly irregular.

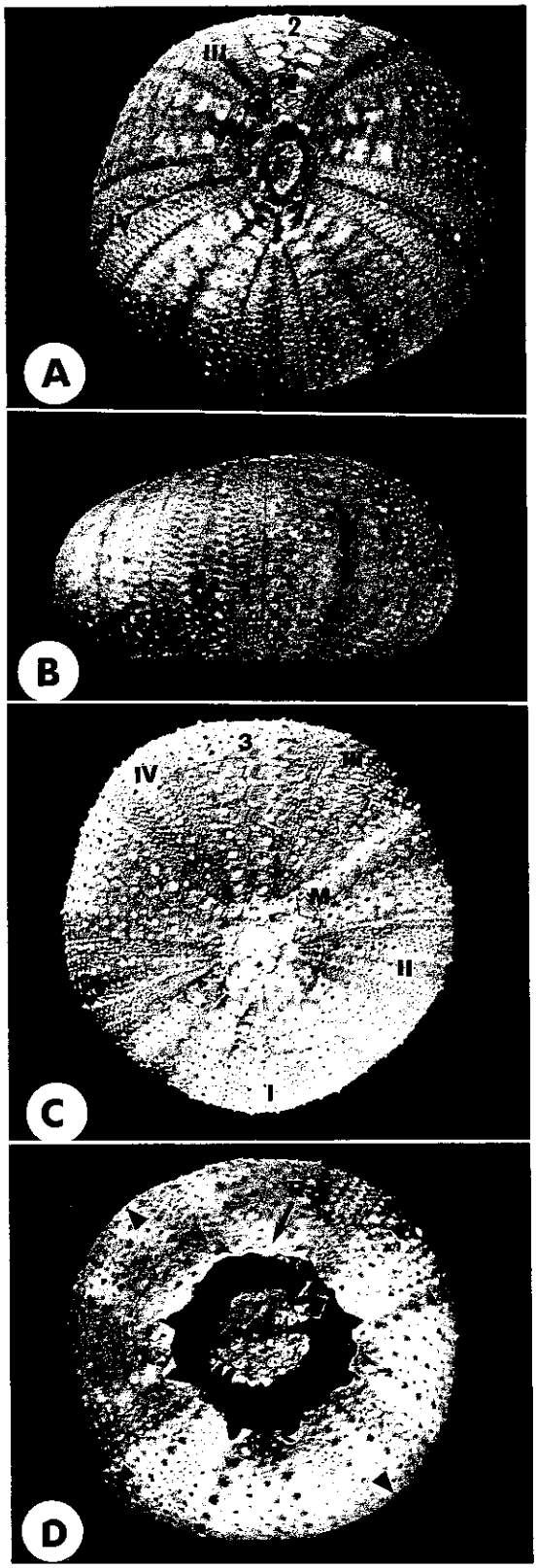

nondamaged ambs were deflected toward the abnormal one. On the whole, it showed a bilateral symmetry and marked skewedness along I-3 axis (Fig. 1C).

(c) "Perfect" and "imperfect" tetramery.—The anatomy of five tetramerous *T. g. elatensis,* collected during the present study, was examined in detail (Table 2). Three of these (nos. 5–7) possessed four ambulacral rays and a four-jawed lantern arranged in a perfect fourfold symmetry which included all skeletal parts. It is here termed "perfect" tetramery. Typical of these individuals was an unusually high H/D ratio (0.60–0.65), compared to the $0.53+/-0.01$ of normal individuals of this subspecies (Dafni 1980). The other tetramers were "imperfect." One (no. 8) was perfectly tetramerous aborally, with a fourfold apical system, consisting of four genital plates and four oculars. Below the ambitus the fourfold symmetry was impaired: one interamb column, at right angles to the madreporite bearing one, was ca. 1.3 wider than the rest at its base. Among the lowermost plates of this interamb was a minute, unpaired plate rudiment, flanked from both sides by interamb plates (Fig. 1D). This individual's normal five-jawed lantern was matched by only four auricles in the peristome edge. Two of these jaws faced the abnormally wider interamb, and one lantern retractor muscle pair was attached to the plate rudiment instead of being attached to an auricle. Two lantern protractor muscle pairs attached to this interamb, on either side of the abnormal retractor, instead of being attached each to a separate interamb. It is probable that one ray, apparently amb IV, was deleted during early postlarval development, together with the two adjoining half-interambulacra. The remaining interamb halves closed in and bridged the gap. The unpaired

←

FIGURE 1. Test configuration of treated and abnormal *T. g. elatensis.* A, B, Aboral and lateral view of individual no. 1, regenerated from amb V immobilization. I to IV, nonaffected amb rays. M, madrepore bearing genital plate Note elongation of the apical system and the inflection of amb I and IV and the bilateral symmetry at V-2 axis. C, individual no. 4, showing similar effects, centered at amb I and deflection of amb II and V. D, oral view of a nonperfect tetramer (no. 8). Dark arrow points at the deleted ray (IV) in which a small, unpaired plate rudiment was noted (R). Dark triangles mark the four active ambulacra.

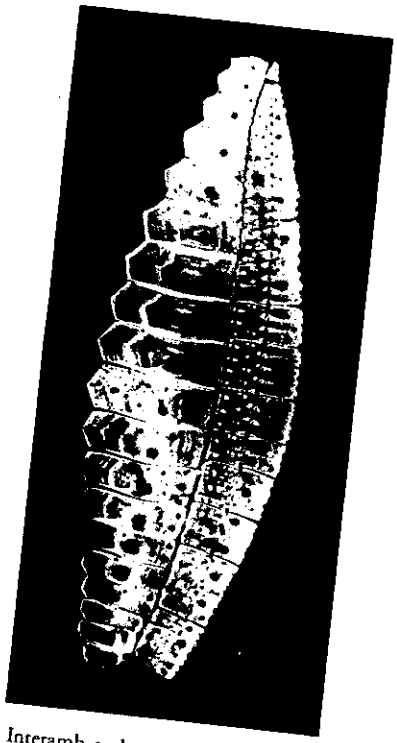

FIGURE 2. Interamb and amb plate rows of a 51-mm *T. g. elatensis*, after charring. The picture was taken in transmitted light to show growth lines.

FIGURE 3. Scanning electron micrograph (SEM) of the interamb plate row aboral end (×100). G, genital plate; O, ocular plate; N, newly added interamb plate; and T, primary spine tubercle of the plate beneath. Note the triangular space available for the next plate.

rudiment, obviously the only remainder of the deleted amb, retained its lantern muscles, while the auricle pair totally disappeared.

Urchin no. 9 was tetrameric aborally, but below the ambitus a 4–5-plate-high fifth amb appeared, equipped with an auricle that was connected via a retractor muscle pair to a normal, five-jawed lantern. Below the ambitus it was truncated and replaced by highly distorted poreless plates. At ambitus level, the plates of the adjacent interamb columns widened toward the gap and closed it entirely. Since the amb rudiment was meridional to the madreporal plate, it was either Loven's amb II or III. This individual's peristome was highly distorted, its aperture being considerably elongated. Both no. 8 and no. 9 had a relatively tall test (H/D = 0.60).

2. Plate edge morphology and micromorphology

(a) Plate edge morphology.—Fig. 2 illustrates a normal meridional column of amb and interamb plates with a growth-line pattern, brought out by charring. Such patterns, and plate-edge configurations of the interamb plates at different parts of the meridional column, allow one to reconstruct the ontogeny of *T. g. elatensis* plates, following a method applied by Deutler (1926) and Märkel (1975, 1976, 1981). According to this reconstruction and evidence provided by Raup (1968), a newly added plate, at the apex, is round-cornered, changing into the triangular form, while fitting into the space provided by the preexistent plates (Fig. 3). At this stage all the plate's margins are curved—convex along the lower latitudinal suture edge and concave in the direction of the apical plates (Figs. 3, 4A). Subsequently, due to the recruitment of a new plate aborally, two more corners are added and the plate becomes pentagonal (Fig. 4B). Now, it is concave in the aboral latitudinal edge, and in the upper half of the interradial sutural edge, and convex at the lower edge and the lower half of the interradial suture. The adradial suture, bordering with the amb plates, assumes a highly serrated appearance due to the convexity of the latter plates (see also Fig. 6). As the plates move further towards the ambitus (Fig. 4C), they strongly elongate laterally, whereas meridional growth is minimal. Their curvature pattern also

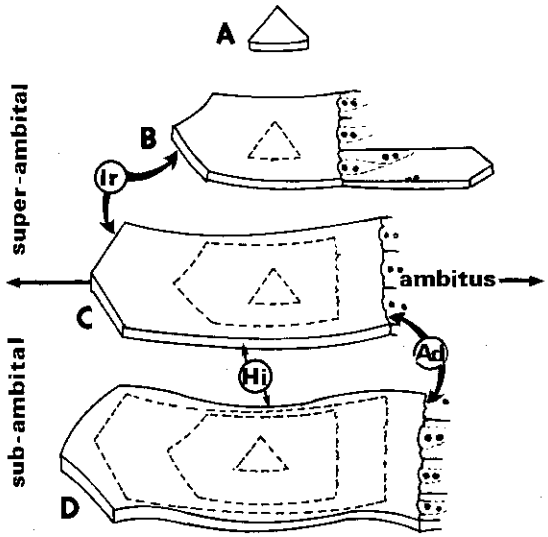

FIGURE 4. Schematic presentation of four ontogenic stages of *T. g. elatensis* interamb plate growth. Previous stages are outlined as growth polygons (broken lines). A, The youngest interamb plate (see also Fig. 3); B, The same plate in a superambital position, showing an amb plate attached at the adradial suture (Ad); C, The plate at an ambital position, showing straightening of the interradial (Ir) edges; and D, At a subambital position, exhibiting reversal of the curvature pattern at the interradial suture, and a wavy suture line horizontally (Hi).

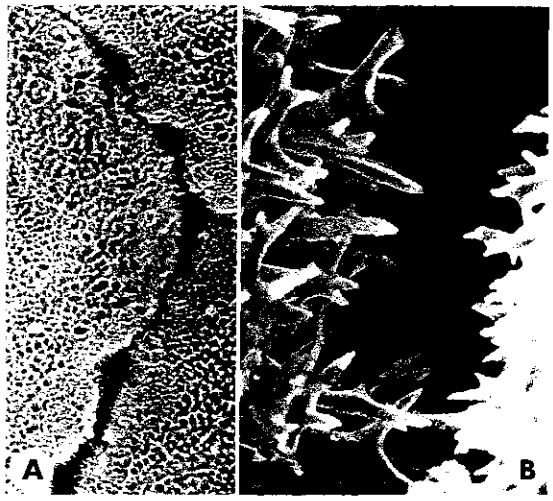

FIGURE 5. Sutural gap of a 20-mm *T. g. elatensis*, formed along the interradial suture, exhibiting extremely elongated and poorly branched trabeculae, growing toward the adjacent plate. A, General view (×40); B, ×400.

changes: The interradial suture straightens, while the aboral and adoral edges retain their former curvature. As the plates reach a subambital position (Fig. 4D) the interradial sutural edges reverse their curvature: the upper half becomes convex and the lower becomes concave. The latitudinal margins develop a wavy pattern, in which the central part retains the former curvature, whereas in their terminal part, toward the interradial and adradial sutures, the curvature is reversed. All earlier stages appear as concentric growth lines in the lowermost plates (Figs. 2, 4D).

Curved plate edges in *T. g. elatensis* invariably occur between plates of unequal outer surface area: the small plate convex toward the large. Exceptions to this rule, of plates slightly unequal but with a straight suture-line, seem to indicate different thickness or porosity. This rule applies also to abnormal *T. g. elatensis* (Dafni 1980, 1983b).

Cases were observed, where the interamb plates of *T. g. elatensis* split into two nearly equal halves, forming a suture with collagen fibers between. Subsequently, the plate halves, surrounded by larger plates, became convex all around, but the newly formed partition was almost straight.

Similar patterns occur in most regular and irregular echinoid species, but were largely different in the flexible tests of the echinothurid urchins, whose plates are imbricated. The peristomial and periproctal plates of stiff-tested echinoids, which are totally embedded in flexible connective tissue, are also all round.

(b) Plate edge microstructure.—Various authors have hypothesized that tensional stresses, developing when the plates are pulled apart at the sutures, encourage sutural growth and calcification (Moss and Meehan 1968; Dafni and Erez 1982). Other investigators suggest that faster-growing suture edges produce slender and well-aligned trabeculae (Kobayashi and Taki 1969; Pearse and Pearse 1975). My attempts to produce tensile stresses in vivo, and to examine the resulting trabeculae, were unsuccessful. However, observations showed that under apparently normal conditions sutural gaps of ca. 0.5 mm frequently appear along the meridional sutures of *T. g. elatensis* individuals. Through the thin epidermal membrane, which covered the gaping sutures, unusually long and parallel collagenous fibers could be seen stretching across the gap. Normally, such gaps were closed within 2–3 wk of the first observation by lateral growth

of the adjoining plates. In one such case, a 20-mm *T. g. elatensis* with a ~1-mm wide gap along the interradial suture was observed for several weeks. After 3 wk the urchin's test was thoroughly cleaned with hypochlorite and the regenerating suture-line prepared for SEM study. The extraordinarily long, slender, and almost nonbranching trabeculae, which had developed during these observations, are shown to extend across the interradial suture (Fig. 5).

(c) Sutural collagenous fibers attachment to the plate.—Figure 6A illustrates a typical tangential decalcified section in a 10-mm *T. g. elatensis* test: a superambital interamb plate surrounded by amb and interamb plates. The width of the sutural collagen band varied, ranging from 50–250 μm (Table 3). The longitudinal sutures, adradial (Ad) and interradial (Ir), had longer and more densely packed fibers (Fig. 6B) than those of the adjacent latitudinal sutures. The interamb latitudinal suture (Hi) had longer fibers only centrally, whereas shorter and less organized fibers showed laterally, in both ends (Fig. 6C).

The fiber-anchoring trabeculae are represented in this section by their decalcified "ghosts" (nonstained areas encircled by collagen fibers). These ghosts were predominantly oval in cross-section, exhibiting their longer axis (a) at the same orientation of the associated fibers, and a shorter perpendicular (b) axis. Table 3 shows that while the trabecular ghosts' areas were similar, their shape (a/b ratio) varied considerably. The ghosts of interradial and adradial sutures (Fig. 6B) had the highest ovateness (a/b ratio of 1.8–2.4), while the terminal trabeculae of the latitudinal sutures (Fig. 6C) had an almost round cross-section (a/b = 1.2). Additional observations, as well as SEM micrographs, confirmed that the oval cross-section of the trabeculae was not due to oblique sectioning or deformation during embedding.

The appropriate model is this of the beam, bending due to the pull exerted by the collagen fibers. Assuming that fiber-associated trabeculae from different sutures do not vary in their mineral composition or specific strength, an estimate of the resistance of the trabeculae to these forces can be derived from calculating the second moment of their cross-sectional area (I) (Wainwright et al. 1976; Emlet 1982). For an ellipsoid beam it is

$$I = a^3 b\pi/64. \quad (1)$$

The interradial suture trabeculae, associated with the longest sutural fibers (250 μm), had the greatest a/b ratio (Table 3) and were stiffest in the direction of the fibers (I = 1,213 μm^4), whereas the trabeculae of the terminal part of the latitudinal suture had the shortest fibers and low stiffness (893 μm^4).

Interamb plates from an equal-sized *T. g. elatensis* were observed with SEM. Figure 7 is a typical example, showing sutural trabeculae and their mode of articulation with the trabeculae across the suture. It shows that the interradial suture (Ir) has longer trabecular ends, that meet the opposite side trabeculae in a rather spacious articulation, while in the terminal part of the latitudinal suture (Hi) the trabecular ends are shorter, and the articulation with the adjacent plate has a more compressed appearance.

3. Phylogeny of regular echinoid test morphology

The relations between ambulacral development and other morphometric indices of regular echinoids are shown in Fig. 8. It shows that the tests of cidaroids, the most primitive echinoids, are nearly spherical, with a high H/D (~0.7), and have an ambitus-line at about mid-height, while the amb width is 4 times narrower than the interamb (or 0.2 of the circumference). In the more advanced orders the ambitus-line tends to be lower, while the ambs reached the largest width (1.4 of the interamb in the camarodonts, i.e., 0.6 of the circumference). The average H/D did not differ significantly among these groups. Assuming an evolutionary progress among these orders (Cidaroida, Aulodonta, Stirodonta, and Camarodonta), Spearman's rank-correlation coefficient (Sokal and Rohlf 1969) was calculated to analyze the various trends (Table 4). To avoid a possible linkage between the indices, the partial correlation (r') was calculated between each pair, while the third index has been kept constant (Weber 1972). To stress the adaptive nature of these indices, the taxonomic factor was ignored in the partial correlation.

The results indicate a significant correlation between ambitus height and the amb system width, adding support to the hypothesis that enhanced activity of the tubefeet causes the flat-

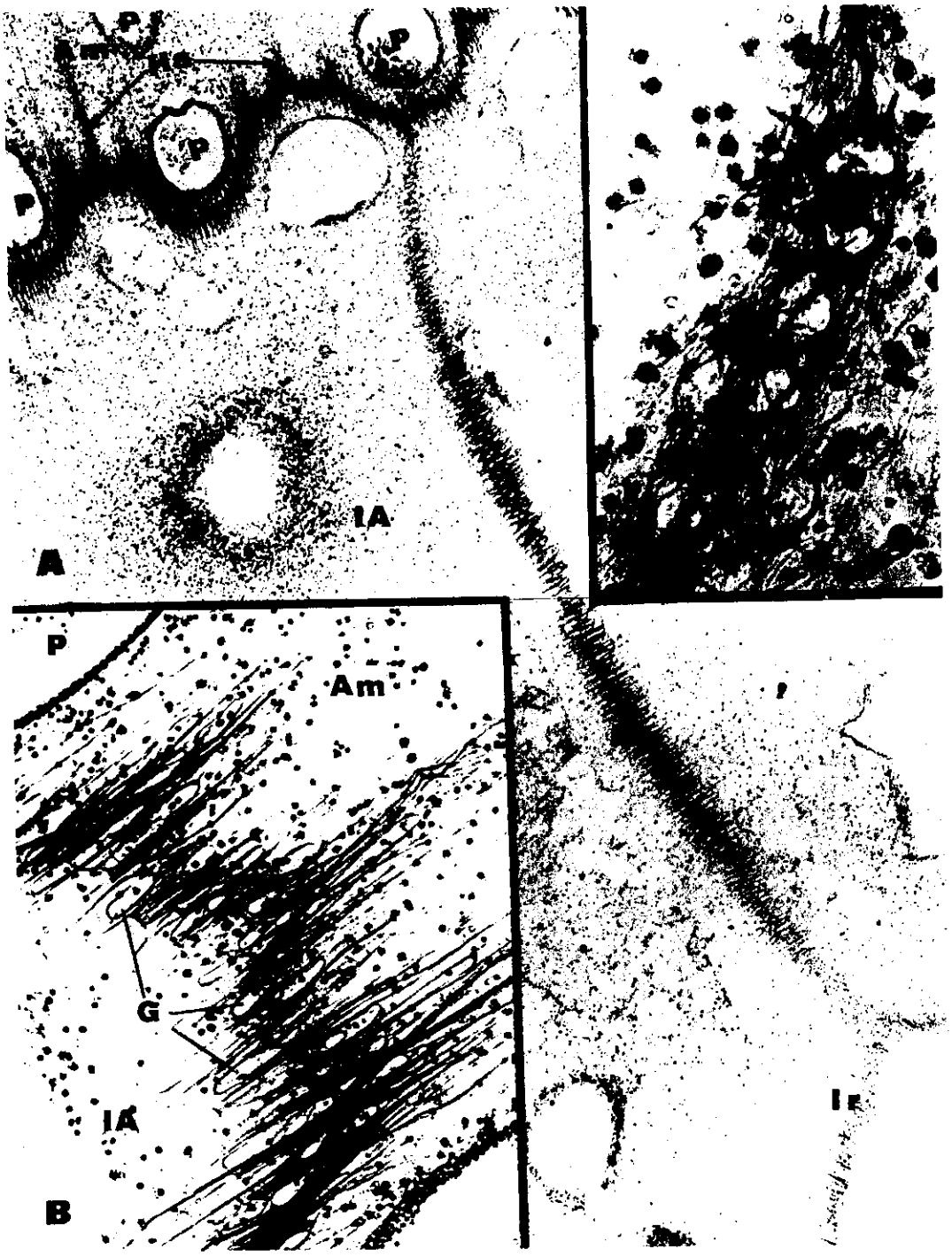

FIGURE 6. Tangential section in a decalcified interamb (IA) plate of a 10-mm *T. g. elatensis*, MSB stain. A, General view (×100) of the longitudinal sutures (adradial [Ad] and interradial [Ir]) and the horizontal sutures (ambulacral [Ha] and interambulacral [Hi]); P = amb tubefeet pores. B, Enlarged adradial suture. C, Terminal part of the Hi suture, showing trabecular ghosts (G); Am = amb plate. B and C are enlarged ×400 and ×600, respectively.

TABLE 3. Length measurement of collagenous fibers and "ghosts" of fiber-associated trabeculae in a decalcified section of a 10-mm *T. g. elatensis* interamb plate illustrated in Fig. 7. Over 30 trabecular ghosts were measured and the means ± SD are given. Differences in "ghost" area were nonsignificant (two-tailed *t*-test, $P > 0.1$). The difference between ovateness of latitudinal and longitudinal "ghosts" was highly significant ($P < 0.05$).

Suture	Fiber band width (μm)	Trabecular ghosts measurements			Ovateness	Second moment (μm⁴)
		Length (a, μm)	Width (b, μm)	Area (μm²)		
Longitudinal:						
Adradial	200	13.6 ± 3.5	7.6 ± 1.8	81.0 ± 28.6	1.8 ± 0.5	941.7
Interradial	250	15.6 ± 8.5	6.5 ± 1.1	79.7 ± 45.3	2.4 ± 1.0	1,213.7
Latitudinal:						
Central part	120	13.0 ± 3.0	9.5 ± 3.3	96.9 ± 32.7	1.4 ± 0.4	1,027.1
Terminal part	50	12.2 ± 2.8	10.1 ± 2.3	96.6 ± 31.6	1.2 ± 0.2	893.2

tening of the adoral half of the test, thus lowering the ambitus line. The low correlation between H/D and ambital height is further reduced when ambulacral width is kept constant. Similarly, the inverse correlation between H/D and amb width was dependent on amb height.

A notable exception to the general correlation between amb system width and ambitus position are mud-inhabiting deep-sea regulars, which are flat adorally and show a sharp lower ambitus-line (Mortensen 1935), or rock-boring camarodonts (e.g., *Echinostrephus*), with test profiles characterized by a flat upper half and tapering adoral side, and a high ambitus-line (Mortensen 1943b). The above correlation would have much improved if such urchins were excluded.

Discussion

Telford's (1985) recent detailed analysis of echinoid test biomechanics adds to previous studies (Moss and Meehan 1968; Nichols and Currey 1968; Currey 1975; Wainwright et al. 1976; Smith 1980, 1984; Strathmann 1981; Emlet 1982) in describing how mechanical design plays an important role in adaptation. The

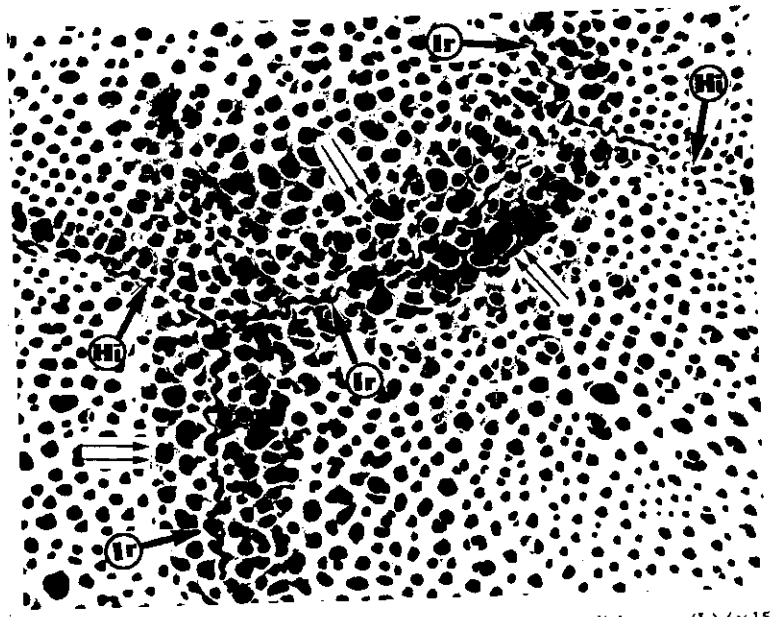

FIGURE 7. SEM of 8-mm urchin (external view), showing the superambital interradial suture (Ir) (×150). An open mesh stereom with longer trabeculae is shown along the suture, whereas horizontally (Hi, terminal part) it has a more condensed appearance. Note the distinct growth line, parallel to the interradial suture (double arrows).

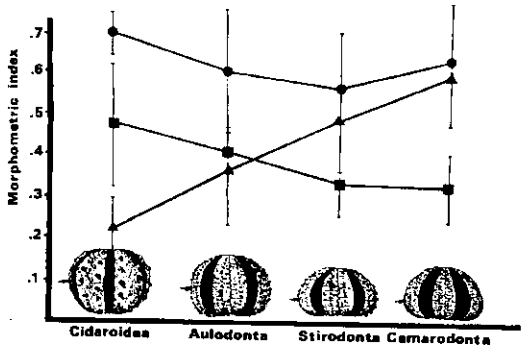

FIGURE 8. The change in several morphometric indices: H/D ratio (●), ambital height relative to test height (■), and ambulacral system relative width (▲) among various regular echinoid orders. The width of the ambulacra was darkened in figures of typical representative species. (No. of species: Cidaroidea, 25; Aulodonta, 27; Stirodonta, 49; Camarodonta, 51) (Error bars: SD). Arrows indicate ambitus position.

question discussed here is how prevailing mechanical forces, external or internal, affect ontogenetic growth, and how significant they are in the morphogenetic process. This has never been analyzed by critical experiments, although the possibility of biomechanical regulation of the echinoid test has been often expressed (Thompson 1917, 1942; Moss and Meehan 1968; Raup 1968; Seilacher 1979; Dafni and Erez 1982; Dafni 1985).

Confirming previous observations (Moore 1935; Ernst 1973; McPherson 1965) on the dependence of the skeletal morphology of regular echinoids on substrate type, the "sand treatment" seems to be the first experimental evidence to support Thompson's (1917) hypothesis. The change in H/D was distinctly higher than predicted by the slight positive allometry of height versus diameter (Dafni 1983b). A biomechanical effect, relaxation of the tubefeet activity, apparently relieves the compressive stresses along the meridional axis (Dafni 1980; Telford 1985), encouraging vertical growth of the coronal plates. An alternative hypothesis, that the reversible H/D change (Table 1B) indicates an elastic flexing of the entire test, rather than a change in the calcification pattern of the individual plates, was refuted in a ^{45}Ca incorporation assay. In this assay, it was found that sand-treated urchins show an entirely different calcification pattern, characterized by a high vertical versus horizontal sutural ratio (v/h). Normally the test plates calcify less in the vertical (=meridional) than in the latitudinal direction, with a v/h ratio of 0.2–0.3. In ambital plates of sand-treated urchins this ratio was >0.6 (Dafni and Erez, in prep.).

Observed changes in urchin test morphology resulting from immobilization of one amb system (Table 2), possibly result from changes in the "force balance" around the test, especially of the forces associated with tubefeet activity. I suggest that the inactivation of the lantern retractor muscle, as seen in individuals 2 and 3, resulted in only a slight skewness, whereas the more pronounced effect, reduction of one amb and lateral deflection of the adjacent ambs (in no. 1), resulted from damaging this amb's ambulacral system, including the radial nerve complex which activates it. The striking similarity between individuals 1 and 4, both having nonfunctional podia in one amb, strongly suggests that inactivation of the podia is the main, if not the only, cause for the observed morphological anomaly (Fig. 1A–C). Similar anomalies were recorded and described in other regular echinoids (Koehler 1924; Jackson 1927; Moore 1974). Moore (1974) attributed these anomalies to mechanical injury at an early postlarval stage that resulted in the loss or inactivation of one or several ambulacra.

There is little doubt that individuals 8 and 9 were initially pentamerous, suffering inactivation and deletion of one amb. Along with it disappeared the interamb half-columns, which flanked the deleted ambs laterally. Asymmetrical growth of the remaining plate columns, and their movement toward the inactivated amb, compensated for the loss, bridged, and finally filled the gap caused by the deletion. Redivision of the entire circumference into four equal ambs produced the tetramerous symmetry. It seems that individual no. 8 suffered the damage at an earlier stage than no. 9, hence the former's relatively more perfect symmetry.

Thus, I suggest that the number of active amb rays largely determines the urchin's symmetry. The normal pentamerous symmetry depends on all five amb rays being functional, pulling at equal force. It is assumed that when a plate is pulled in one direction, it will grow more in the opposite direction, where tension is

TABLE 4. Rank-correlation coefficients (Spearman's r) of several morphometric parameters for 147 contemporary and fossil hard skeleton regular echinoid species, representing four orders. r' values result from partial correlation. Significance of trends was tested by a t-test, with a null hypothesis of $r = 0$ (NS = nonsignificant).

Compared parameters	Correlation coefficient and significance	
	Corr. coef. (r)	Partial correlation (r')
Order vs. H/D ratio	−0.90 (NS)	Not calculated
Order vs. ambital height	−0.525 ($P < .001$)	Not calculated
Order vs. ambulacral width	+0.657 ($P < .001$)	Not calculated
H/D vs. ambital height	+0.219 ($P < .01$)	+0.149 (NS)
H/D vs. ambulacral width	−0.199 ($P < .05$)	−0.118 (NS)
Ambital height vs. amb width	−0.443 ($P < .01$)	−0.442 ($P < .01$)

highest (Dafni and Erez 1982; Dafni 1985), so that its center shifts toward the pulling force. Hence, unbalanced forces around the test circumference cause intact ambulacra to shift latitudinally, curving to the direction of the deleted amb. The phenomenon of curving of nondamaged ambs toward the damaged ones is a common occurrence in teratological urchins which suffer injury (Koehler 1924; Jackson 1927; Moore 1974).

While studying five "perfect" tetramers of the rock-inhabiting regular echinoid *Arbacia punctulata,* Jackson (1927) noticed that they were relatively taller (calculating the H/D ratio from his figures, I found it $0.62 \pm / -0.06$, significantly higher than the normal ratio, reported by the author as 0.51). Similarly, the H/D of tetramers nos. 5–9 (Table 2), perfect and imperfect, was $0.62 + / -0.02$, compared to $0.53 + / -0.01$, recorded for normal *T. g. elatensis* of the same size order. Considering that tetramers have fewer podia interacting with the substrate (ca. ⅝ of the normal), this observation supports the hypothesis tested in the sand experiment, i.e., that feeble adherence ontogenetically results in taller individuals.

The analogy between soap-bubble curvature and plate-edge morphology is also relevant to our discussion. A soap bubble is an air-filled inclusion, surrounded by a thin membrane, whose area is minimized by surface tension. The bubble's morphology is, therefore, mechanically determined, in equilibrium with the external pressure. According to Plateau's laws (Stevens 1976), the inner hydrostatic pressure is inversely related to the bubble's radius. Equal bubbles share equal inner pressures and when joining, the intermediate partition runs straight. The partition wall between unequal bubbles convexes toward the larger bubble, in which hydrostatic pressure is lower. The curvature radius of the partition wall (R_c) can be derived from individual bubbles' radii (R_1 and R_2), using the following equation (Stevens 1976):

$$R_c = R_1 \times R_2/(R_1 - R_2). \qquad (2)$$

In equal bubbles R_c is infinitely large, i.e., the partition wall is straight. The same rule applies to three and more bubbles (Fig. 9).

Raup (1968) maintained that "though the analogy between the soap-bubble arrays and actual plate configuration is a very tempting one, we must be cautious in reasoning from one to the other." The main obstacle is probably that an echinoid plate is ordinarily viewed as a solid object, unable to flex its surface in a bubble-like manner. But this obstacle can be easily lifted by accepting Moss and Meehan's (1967, 1968) argument that the plate calcification is secondary, occurring "within a mesodermal body-wall capsule, which is itself expanding as response to the growth of the enclosed body mass." The flexible capsule, consisting of an outer epidermal "ectotest," an "endotest" bordering the coelom, and partitions composed mainly of sutural fibers, shows best in decalcified tests (Moss and Meehan 1967). The capsule retains its form even after the entire plate has been decalcified, provided it remains submerged in liquid. Since the plate capsula is an inclusion containing fluid-like syncytic tissue, the stroma, that fills the interstices of the stereom, it is liable to harbor distinct hydrostatic pressures as well as an outer surface tension.

As suggested by this analogy, the echinoid plate behaves elastically as far as growth is concerned. Its shape at any given stage reflects the mechanical properties of the capsule. Reversal of the plate-edge curvature occurs, according to this model, when a formerly smaller plate becomes

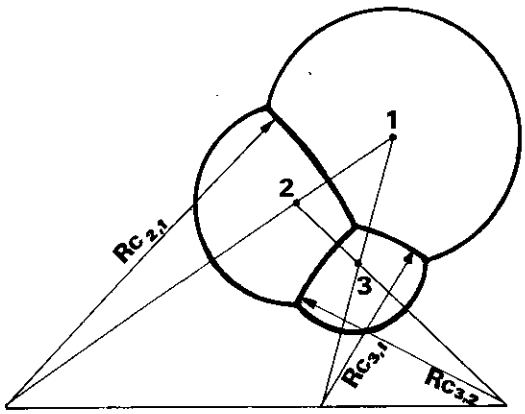

FIGURE 9. Three bubbles, separated by curved walls. Rc, curvature radii of the partition walls, Rc 2, 1 for the wall between bubbles 1 and 2, etc. (adapted from Stevens 1976).

larger than its neighbors, with the relation between their inner pressure reversed. Since no calcareous material is resorbed in the plate margins (Jensen 1972; Märkel 1975, 1976), pattern reversal can take place only in faster-growing sutures of plates that crossed the plate midline, while the same plates' nongrowing edges, such as the central part of the latitudinal sutures, retain their "anachronistic" curvature and the wavy pattern forms (Fig. 4D).

Change in plate curvature of accidentally splitted plates is another argument for the inner pressure hypothesis. It is hard to envisage any factor which may have changed by splitting, other than the relation between the plates' inner volumes and their individual volume/surface area ratio.

Suture lines of other test forming organisms (foraminifers, coccolithophorids, plate-covered fish) usually do not conform to this model. Body shapes of sedentary colonial organisms (corals, barnacles, or bryozoans) exhibit noncurved "close-packing" patterns (Stevens 1976). Bubble-like curvature occurs, however, in insect wing "cells" (Neuroptera, Odonata, etc.). Since insect wings arise as notal flaps of the outer body wall, shaped when in a wet state, it is safe to assume that each "cell" is indeed a membrane-covered hollow inclusion, separated by cross-veins of tracheal origin (Ettershank and Ghent 1972). To conclude, the soap-bubble model is applicable to structures that form as hollow inclusions surrounded by flexible membranes, with or without internal mineral content.

If the Moss and Meehan (1968) approach is accepted, minute sutural gaps that are often seen in SEM pictures are indispensable to accommodate trabecular growth. It is likely that in the growing tests there are wider gaps, due to the intensive somatic growth. Trabeculae respond to this situation by growing faster in well-aligned orientation. Sutural gaps of nongrowing urchins are expected to be narrow and trabeculae short and stubby. This hypothesis is supported by unusually slender and nonbranching trabeculae, apparently caused by an abnormally wide gap (Fig. 5).

Figures 6 and 7, as well as measurements shown in Table 3, suggest that the longest and more densely packed collagenous fibers, shown along the longitudinal sutures, co-occur with longer sutural trabeculae. Combining this evidence with data showing that these sutures calcify at a faster rate than the latitudinal (those growing vertically) (Dafni and Erez 1982, in prep.), and that the unusually wide gaps occur predominantly in the longitudinal sutures, I suggest that the latter are under stronger tension, while the latitudinal sutures are more compressed. The last conclusion is in perfect accord with Telford's (1985) biomechanical analysis.

The fiber-associated "trabecular ghosts" of the more tensed longitudinal sutures are strongly oval, with a cross-sectional second moment higher than in the presumably compressed latitudinal sutures. This further supports the argument that the trabecular length, branching, and cross-section pattern are affected by the stresses that develop along the sutures.

Without denying a possible effect of external forces, several internal force-producing muscular and elastic connective tissue elements are proposed to form a mechanical array of forces that controls the normal growth and morphogeny of echinoid tests. These elements are included in an integrated biomechanical model (Fig. 10). The adopted paradigm is that of a tensional sphere, the bubble-like "pneu" (Otto and Trostel 1967), which is supported internally by the contained liquid pressure and counterbalanced by an outer surface tension. A pneu structure grows when the internal pressure exceeds the external surface tension. This is a principle common to all organisms with a "hydrostatic skeleton" (Chapman 1958). The same principle was adopted by

Moss and Meehan (1968) for description of the human neurocranium and echinoid test growth: Since both structures consist of articulated mineral plates, the expansion of the inner mass generates sutural tension, which is compensated by peripheral growth of the plates. Therefore inner liquid pressure is the model's basic component (1).

Although there is no published evidence that internal hydrostatic pressures within the coelom exceed the external ones, internal higher pressure may be derived from Donnan's effect (Prosser and Brown 1961): Macromolecules, mainly proteins, concentrate in the perivisceral fluid (Giese 1966), inducing the entrance of smaller ions through the semi-permeable body integument, followed by water influx. This influx of water is balanced by tension developed in the body wall. This tension probably produces sutural gaping. Higher hydrostatic pressures that develop in other internal compartments (e.g., tubefeet, lumen, and gut), also induce water movement to the coelom, forming occasional coelomic pressures. Transient increases in pressure occur when all tubefeet contract simultaneously (Buchanan 1969). It has been demonstrated that an entire, decalcified test retains its former inflated shape without the skeletal support when submerged in fluid (Dafni, unpublished). This is probably because of the tensility of the outer body wall, that presses the inner liquid, forming a flexible pneu.

One may speculate that growth lines, alterations between slow and rapidly growing stereom (Smith 1980), reflect changes in inner pressure conditions. Intensive growth is associated with higher internal pressures and sutural tension, while periods of slow growth are characterized by low internal pressures. This is probably when the entire structure may rely on its mineral framework and so compression develops at all sutures.

Tubefeet attachment (its effect on test morphology was tested here) is another component of this model (2). Although the actual forces involved were never measured for echinoids, their magnitude can be estimated from Paine's (1926) measurements of starfish tubefeet adherence (19 g/mm^2). Sharp and Gray (1962) noted that the tubefeet suction discs of hard-bottom species are considerably larger than those of soft-bottom echinoids, while Lissner (1983) showed that in

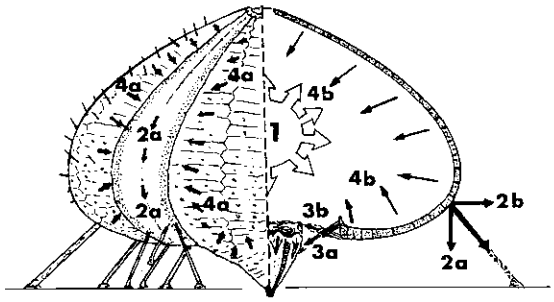

FIGURE 10. Schematical presentation of the proposed model, showing the various force components involved in echinoid morphogenesis, side view (left) and section (right): (1) expansion of the inner mass; (2) forces produced by the tubefeet (2a, 2b, vector component discussed in the text); (3) lantern muscles (3a, 3b, retractor and protractor, respectively); (4) mesenterial threads activity, pulling at the plates in the plate level (4a) or centripetally (4b). Vectors' size and direction are arbitrary.

echinoids adapted to strong water motion more podia are used for attachment. Although tubefeet spread out in all directions, the resultant vector of each amb ray points outward with a distinct downward inclination (Thompson 1917). It is therefore divided here into two vector components: (2a) a vector active along the amb meridian and another one (2b), pointing radially outward. Since tubefeet pull the plates to the substrate, the former component obviously pulls the plates downward (Moss and Meehan 1968), while the latter causes test flattening (Thompson 1917).

The lantern muscles, the retractor (3a) and the protractor (3b), connect the lantern with the lowermost coronal plates. Their possible mechanical effect on the corona—pulling together the peristome's rims—remains to be demonstrated.

The mechanical activity of the intestine mesenterial threads, another tethering component (4) was suggested by Dafni and Erez (1982), who found their distribution patterns correlating with the differential growth pattern of the interamb plates. It is suggested that these threads influence in two different ways, application of (4a) force vectors that affect the interamb plates' growth in a differential pattern (Dafni and Erez 1982, fig. 3), and (4b), tying together the ineramb plates and pulling them in a centripetal direction (Fig. 10). This component counterbalances the outward expansion of the test and simultaneously causes its flattening. It has been dem-

onstrated that aboral depressions, shown in deformed *T. g. elatensis,* were obviously facilitated by these threads' activity (Dafni 1983b). It has been suggested that these threads are homologous with the unique meridionally aligned muscle sheets of flexible-tested echinothurids (Dafni 1983b).

The collagenous sutural fibers probably play a passive role in this force balance. They resist forces produced by the previously mentioned elements, contributing thereby to the mechanical stability of the test (Moss and Meehan 1967; Strathmann 1981). Recent findings that echinoderm collagen may undergo controlled changes in its tensility (Motokawa 1983; Wilkie 1984) may suggest a more active involvement of these fibers in the growth process (i.e., yielding in rapidly growing sutures and hardening in the nongrowing sutures).

Although proposed for *T. g. elatensis,* the model may be applicable to all regular echinoids with stiff skeletons, and to a certain extent also to irregulars. Regular echinoids vary, however, in their test thickness and architectural design (Ebert 1982; Telford 1985). It is therefore probable that the relative importance of each of this model's components also differs among the taxa. A quantitative assessment of the mechanical forces involved in this model will be a step toward explaining the morphological variation among different echinoid species.

The phylogenetic implications of the model are based on the assumption that the same processes may apply to both ontogeny and phylogeny. The possible reason for this is that constraints shown during ontogeny frequently are those dominating the phylogeny of the group. For instance, it has been demonstrated that irregular echinoid postlarvae undergo ontogenetic development that closely simulates the evolution of the group (Gordon 1926). Apart from the obvious influence of inherited genetic information on the organism's morphology, it is likely that the biomechanical interaction between the organism's various tissues during ontogeny largely determines its shape, with a contributing effect of the external environment.

The morphometric analysis showed that, while H/D ontogenetically correlated with amb activity, it was independent at the phylogenetic level (Table 4). This is in accordance with the observations that some soft-bottom echinoids have H/D ratios lower than predicted by the above hypothesis (e.g., *Diadema*). In deformed *T. g. elatensis,* flattening was apparently caused by inner tethering (Dafni 1983b). Inner tethering also characterizes the evolution of the clypeastroids (Seilacher 1979). A low ambitus line is, however, an evolutionary trend well-correlated with the development of the amb system.

The most important adaptation in regular echinoids' evolution is related to the ambulacral system (Kier, in Moore 1966). Paleozoic echinoids (e.g., *Eothuria*) were apparently flexible, with tiny podia and a tendency to elongate in the vertical axis. This is probably linked to a sea-cucumber-like inclination on the seabed. Subsequent evolution shifted the podia toward the adradial sutures, increased the number and density of podia by forming compound amb plates and their concentration as ventral phyllodes (Smith 1984). Many primitive echinoids were nearly globular, with a high ambitus line, and apparently had a feeble contact with the substrate. Cuénot (1948) reconstructed the habitat of the Carboniferous *Melonechinus* by comparing it to the present-day globular genera *Amblypneustes* and *Holopneustes*. Both are known to live cradled among algae in undisturbed habitats, a habit which is reflected in their poorly developed tubefeet pores (Smith 1978).

Soft-bottom regular echinoids are usually flat ventrally. Such flattening is common also among soft substrate reclining stony corals or molluscs (Seilacher 1984), apparently aimed to prevent sinking in the extremely unstable soft habitat. It could also aid locomotion by bringing more spines to lean on the sediment. This is explicitly shown by the extant deep-sea-mud-inhabiting stirodonts, *Hebrocidaris, Dialithocidaris, Podocidaris, Baueria,* and *Heteropodia* (illustrated by Mortensen 1935), and fossil holectypoids (Family Discodeidae), all characterized by a sharp ambital edge. Biomechanically, this may be caused by inner tethering and the test yielding to its own weight.

The emergence of the Irregularia—the most significant development in echinoid evolution—was accomplished through several morphogenetic steps that took place within relatively short

periods (Kier 1982). Several of these steps are reflected in abnormal regular echinoids and conform to this model:

(a) Flattening of the test is associated with the cessation of vertical shift of plates across the ambitus line, and its fixation. Since this occurs in a relatively early ontogenetic stage in contemporary clypeastroids, it involves a different allometry of adoral and aboral plates (Seilacher 1979).

(b) Bilateral symmetry was obtained in two steps—periproct departure from the apical system and its down-shifting, and the differentiation of the amb system into an aboral half, forming the petaloid and adoral half with scattered amb podia. Both steps were accommodated in perfectly round early irregulars. The bilateral symmetry in the deformed regulars, teratological or resulting from injury, resulted from inactivation of one amb. Decreased mechanical activity of the frontal amb of the irregulars may have caused this effect in the phylogenetic level.

(c) Petaloid ambulacra, another feature of the irregulars, produced by relatively narrowing of the amb system above the ambitus, bears a remarkable similarity to "ambulacral pinches" shown in deformed *T. g. elatensis* (Dafni 1980, 1983b). This may be due to a possible biomechanical effect (Dafni and Erez, in prep.).

Acknowledgments

I wish to thank Prof. F. D. Por and Dr. J. Erez for their advice and encouragement. The H. Steinitz Marine Biology Laboratory staff is thanked for help provided throughout this study. The morphometric survey was carried out in the Geological and Paleontological Institute of the University of Tübingen, FRG, in the framework of the Sonderforschungsbereich 230 (Natürlische Konstruktionen). T. A. Ebert, J. M. Lawrence, D. Nichols, A. Seilacher, and A. Diamant read drafts of this paper, and it greatly benefited from their constructive criticism. Photographs were taken by A. Niv.

Literature Cited

BENSON, R. H. 1975. Morphological stability in Ostracods. Bull. Am. Paleontol. *65*:13–46.

BONNER, J. T., ED. 1961. On growth and form, by D. W. Thompson. Cambridge Univ. Press; Cambridge.

BUCHANAN, J. B. 1969. Feeding and control of volume within the test of regular sea urchins. J. Zool. Lond. *159*:51–64.

CHAPMAN, G. 1958. The hydrostatic skeleton in the invertebrates. Biol. Rev. Cambridge Phil. Soc. *33*:338–364.

CULLING, C. F. A. 1974. Handbook of histopathological and histochemical techniques. 3d ed. Butterworths; London.

CUÉNOT, L. 1948. Echinodermata. Pp. 1–363. In: Grassé, P. P., ed. Traité de Zoologie XI. Masson; Paris.

CURREY, J. D. 1975. A comparison of the strength of echinoderm spines and mollusc shells. J. Mar. Biol. Ass. UK. *55*:419–424.

DAFNI, J. 1980. Abnormal growth patterns in the sea urchin *Tripneustes* cf. *gratilla* (L.) under pollution (Echinodermata: Echinoidea). J. Exp. Mar. Biol. Ecol. *47*:259–279.

DAFNI, J. 1983a. A new sub-species of *Tripneustes gratilla* (L.) from the northern Red Sea (Echinodermata: Echinoidea: Toxopneustidae). Isr. J. Zool. *32*:1–12.

DAFNI, J. 1983b. Aboral depressions in the tests of the sea urchin *Tripneustes* cf. *gratilla* (L.) in the Gulf of Eilat, Red Sea. J. Exp. Mar. Biol. Ecol. *67*:1–15.

DAFNI, J. 1985. Effect of mechanical stress on the calcification pattern in regular echinoid skeletal plates. Pp. 233–236. In: Keegan, B. F. and B. D. S. O'Connor, ed. Echinodermata: Proc. 5th Int. Echinoderm Conf. Galway, September 1984.

DAFNI, J. AND J. EREZ. 1982. Differential growth in *Tripneustes gratilla* (Echinoidea). Pp. 71–75. In: Lawrence, J. M., ed. Echinoderms: Proc. Int. Conf. Tampa Bay, September 1981.

DAFNI, J. AND J. EREZ. In prep. Skeletal calcification patterns in the sea urchin *Tripneustes gratilla elatensis*.

DEUTLER, F. 1926. Über das Wachstum des Seeigelskeletts. Zool. Jb. (Anat.). *48*:119–200.

EBERT, T. A. 1982. Longevity, life history, and relative body wall size in sea urchins. Ecol. Monogr. *52*:353–394.

EMLET, R. B. 1982. Echinoderm calcite: a mechanical analysis from larval spicules. Biol. Bull. *163*:264–275.

ERNST, G. 1973. Aktuopaläontologie und Merkmalsvariabilität bei mediterranen Echiniden und Rückschlusse auf die Ökologie und Artumgrenzung fossiler Formen. Paläontol. Z. *47*:188–216.

ETTERSHANK, G. AND R. L. GHENT. 1972. Insecta. Pp. 552–613. In: Marshall, A. J. and W. D. Williams, eds. Textbook of Zoology: Invertebrates. MacMillan; London.

GIESE, A. C. 1966. On the biochemical constitution of some echinoderms. Pp. 757–796. In: Boolootian R. A., ed. Physiology of Echinodermata. Interscience; New York.

GORDON, I. 1926. The development of the calcareous test of *Echinocardium cordatum*. Phil. Trans. *215B*:255–313.

GUTMANN, W. F. 1977. Phylogenetic reconstruction, theory, methodology and application to chordate evolution. In: Hecht, M. K., P. C. Goody, and B. M. Hecht, eds. Major patterns in vertebrate evolution. Nato Adv. Stud. Inst. *14A*:645–669.

HYMAN, L. H. 1955. The Invertebrates. Vol. 4. Echinodermata, the Coelomate Bilateria. 763 pp. McGraw-Hill; New York.

JACKSON, R. T. 1927. Studies of *Arbacia punctulata* and allies and of non-pentamerous echinids. Mem. Boston Soc. Nat. Hist. *8*:435–565.

JENSEN, M. 1972. The ultrastructure of the echinoid skeleton. Sarsia. *48*:39–48.

KIER, P. M. 1982. Rapid evolution in echinoids. Palaeontology. *25*:1–10.

KOBAYASHI, S. AND J. TAKI. 1969. Calcification in the sea urchins.1. A tetracyclin investigation of growth of the mature test in *Strongylocentrotus intermedius*. Calc. Tiss. Res. *4*:210–223.

KOEHLER, R. 1924. Anomalies, irregularités et déformations au test chez les echinids. Ann. Inst. Oceanogr. Monaco, N.S. *1*:159–480.

LISSNER, A. L. 1983. Relationship of water motion to shallow water distribution and morphology of two species of sea urchins. J. Mar. Res. *41*:691–709.

MÄRKEL, K. 1975. Wachstum des Coronar skelettes von *Paracentrotus lividus* Lmk. Zoomorphologie. *82*:259–280.

MÄRKEL, K. 1976. Struktur und Wachstum des Coronarskelettes von *Arbacia lixula* Linne (Echinodermata: Echinoidea). Zoomorphologie. *84*:279–299.

MÄRKEL, K. 1981. Experimental morphology of coronar growth in regular echinoids. Zoomorphology. *97*:31–52.

MCPHERSON, B. P. 1965. Contribution to the biology of the sea urchin *Tripneustes ventricosus*. Bull. Mar. Sci. *15*:228–244.

MOORE, H. B. 1935. A comparative study of the biology of *Echinus esculentus* in different habitats. II. J. Mar. Biol. Ass. U.K. *20*:109–128.

MOORE, H. B. 1974. Irregularities in the test of regular sea urchins. Bull. Mar. Sci. *24*:545–560.

MOORE, R. C., ED. 1966. Treatise on Invertebrate Paleontology. Pt. U. Echinodermata. 695 pp. Geol. Soc. Am. and Univ. Kansas Press.

MORTENSEN, T. 1928. A monograph of the Echinoidea. *1*. Cidaroidea. 551 pp. C.A. Reitzel; Copenhagen.

MORTENSEN, T. 1935. A monograph of the Echinoidea. *2*. Stirodonta. 647 pp. C.A. Reitzel; Copenhagen.

MORTENSEN, T. 1940. A monograph of the Echinoidea. *3*(1). Aulodonta. 370 pp. C.A. Reitzel; Copenhagen.

MORTENSEN, T. 1943a. A monograph of the Echinoidea. *3*(2). Camarodonta. 533 pp. C.A. Reitzel; Copenhagen.

MORTENSEN, T. 1943b. A monograph of the Echinoidea. *3*(3). Camarodonta. 446 pp. C.A. Reitzel; Copenhagen.

MOSS, M. L. AND M. MEEHAN. 1967. Sutural connective tissues in the test of an echinoid. *Arbacia punctulata*. Acta Anat. *66*: 279–304.

MOSS, M. L. AND M. MEEHAN. 1968. Growth of the echinoid test. Acta Anat. *69*:409–444.

MOTOKAWA, T. 1983. Mechanical properties and structure of the spine-joint central ligament of the sea urchin, *Diadema setosum* (Echinodermata, Echinoidea). J. Zool. Lond. *201*:223–235.

NICHOLS, D. AND J. D. CURREY. 1968. The secretion structure and strength of echinoderm calcite. Pp. 251–261. In: McGee-Russell, S. M. and K. F. A. Ross, eds. Cell Structure and Its Interpretation: Essays Presented to J. R. Baker. Edward Arnold; London.

OTTO, F. AND R. TROSTEL. 1967. Tensile Structures. Vols. *1, 2*. MIT Press; Cambridge, Mass.

PAINE, V. L. 1926. Adhesion of the tube feet in starfish. J. Exp. Zool. *45*:361–366.

PEARSE, J. S. AND V. B. PEARSE. 1975. Growth zones in the echinoid skeleton. Am. Zool. *15*:731–753.

PROSSER, C. L. AND F. A. BROWN. 1961. Comparative Animal Physiology. 2d ed. Saunders: Philadelphia.

RAUP, D. M. 1968. Theoretical morphology of echinoid growth. J. Paleontol. *42*:50–63.

SEILACHER, A. 1979. Constructional morphology of sand dollars. Paleobiology. *5*:191–221.

SEILACHER, A. 1984. Constructional morphology of bivalves: evolutionary pathways in primary versus secondary soft-bottom dwellers. Palaeontology. *27*:207–237.

SHARP, D. T. AND I. E. GRAY. 1962. Studies on factors affecting the local distribution of two sea urchins, *Arbacia punctulata* and *Lytechinus variegatus*. Ecology. *43*:309–313.

SMITH, A. B. 1978. A functional classification of the coronal pores of regular echinoids. Palaeontology. *21*:759–790.

SMITH, A. B. 1980. Stereom microstructure of the echinoid test. Spec. pap. Palaeontol. Palaeontol. Assoc. Lond. *25*:1–81.

SMITH, A. B. 1984. Echinoid Palaeontology. 190 pp. Allen & Unwin; London.

SOKAL, R. R. AND F. J. ROHLF. 1969. Biometry. 776 pp. W. H. Freeman; San Francisco.

STEVENS, P. S. 1976. Patterns in Nature. 240 pp. Penguin; Middlesex.

STRATHMANN, R. R. 1981. The role of spines in preventing structural damage to echinoid tests. Paleobiology. 7:400–406.

TELFORD, M. 1985. Domes, arches and urchins: the skeletal architecture of echinoids (Echinodermata). Zoomorphology. *105*: 114–124.

THOMPSON, D. W. 1917. On Growth and Form. 1st ed. 794 pp. Cambridge Univ. Press; Cambridge.

THOMPSON, D. W. 1942. On Growth and Form. 2d ed. 1116 pp. Cambridge Univ. Press; Cambridge.

WAINWRIGHT, S. A., W. D. BIGGS, J. D. CURREY, AND J. M. GOSLINE. 1976. Mechanical Design in Organisms. Edward Arnold; London.

WEBER, E. 1972. Grundriss der Biologischer Statistik. 706 pp. Fischer Verlag; Stuttgart.

WILKIE, I. C. 1984. Variable tensility in echinoderm collagenous tissues: a review. Mar. Behav. Physiol. *11*:1–34.